

Pulsed Battery Discharge in Communication Devices*

C.F. Chiasserini[†]

Dipartimento di Elettronica
Politecnico di Torino – Italy
chiasserini@polito.it

R.R. Rao

Department of Electrical and Computer Engineering
University of California at San Diego
rrao@ucsd.edu

Abstract

The overall objective of this work is to explore ways in which the energy efficiency of communications can be enhanced through the use of communication protocols that exploit the charge recovery mechanism inherent to many secondary storage batteries. In the first part of this paper, we summarize the behavior of electrochemical energy cells. We compile results that pertain to the capacity of a cell and its dependence on the intensity of the discharge current. The phenomenon of charge recovery that takes place under bursty or pulsed discharge conditions is identified as a mechanism that can be exploited to enhance the capacity of a cell. The bursty nature of many data traffic sources suggests that there may be a natural fit between the two. In the second part of this manuscript, we explore this synergy by developing a stochastic model that tracks charge recovery in conjunction with bursty discharges due to transmissions driven by Bernoulli arrivals. We derive the resulting capacity advantage relative to constant discharge as a function of the burstiness of the arrival for two discharge scenarios.

1 Introduction

Portable devices must often rely on battery energy to conduct communications. A simplified view of a portable radio device is shown in Fig. 1, where the *radio* part consists of a baseband/digital section, a RF section and a power amplifier, each of which requires a different power supply [14]. Typically the baseband and RF sections consume a constant level of power but the power amplifier draws a much greater amount of power during transmissions. The power supply unit may be a replaceable (*primary*) battery or a recharge-

able (*secondary*) one. It is quite obvious that features such as a long lifetime, light weight and a small size are highly desirable. For these reasons, energy consumption management has become a critical issue in portable telecommunications systems.

Various MAC protocols [21, 20, 3] and schemes for power management control during transmissions [1, 15] have been proposed in the literature to conserve as much energy as possible. The approach presented here differs from the previous work in that the aim of this paper is to understand battery behavior and exploit the bursty nature of telecommunications sources to maximize the energy delivered by the battery, i.e., the number of packets transmitted by the user terminal.

Typically power is drained from cells using a constant current discharge; however, if a pulsed current discharge is adopted, significant improvements seem possible [13, 18, 8, 11, 10, 17]. In particular the time period that elapses from when the battery is fully charged to when it is considered discharged can be significantly extended by draining power for short time intervals followed by idle periods. During the idle periods, also called the *relaxation* time, the battery can partially recover the charge lost while delivering the current impulse.

In this paper, we develop a model for cell behavior that captures the dynamics of the recovery mechanism and study the actual gain derived under stochastic pulsed discharge induced by Bernoulli arrivals. Two different pulsed discharge modes are studied and we derive the resulting capacity advantage relative to constant discharge.

The remainder of the paper is organized as follows: Sect. 2 discusses the most relevant characteristics of the battery behavior; Sect. 3 presents an analytical model of the battery performance under pulsed current discharge; Sect. 4 shows results; and, finally, Sect. 5 concludes the paper and identifies further topics of research.

2 Battery Behavior

Batteries store chemical energy and deliver electrical energy through an electrochemical conversion process. A battery consists of one or more *cells*, organized in an array. Each cell consists of an anode, a cathode and the electrolyte that separates the two electrodes and allows the transfer of electrons, as ions, between them [13].

The ideal electrochemical cell should be extremely light, able to provide an infinite amount of energy, and to handle all

*Supported by NSF under grant CCR 9714651.

[†]On leave at the Center for Wireless Communications, San Diego.

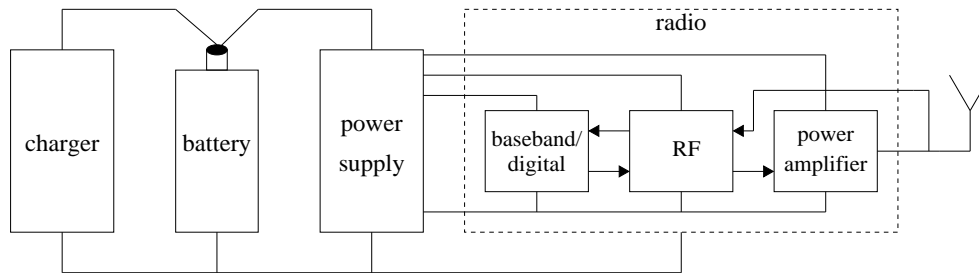


Figure 1: Building blocks of a portable radio system.

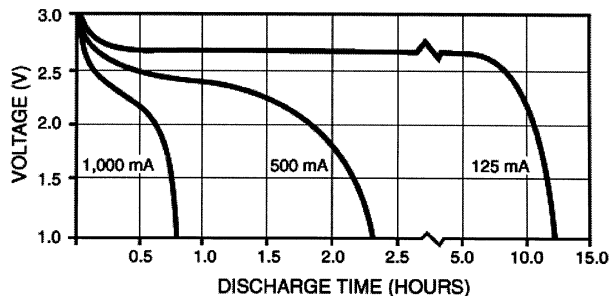


Figure 2: Discharge behavior of a lithium-ion cell with $V_{OC}=3$ V and $V_{cut}=1.0$ V [6].

the desired levels of power. In practice, the energy that can be obtained from a cell is limited by the quantity of active material contained in the cell. Therefore, the lighter the cell, the smaller its capacity. In fact there is a measure of the capacity of a cell that is a function only of the type and mass of the electrodes and electrolytes. This is the theoretical capacity. While one can not hope to exceed this capacity, the challenge in cell design is to come close to this capacity. In practice, the delivered specific energy greatly depends on the intensity of the discharge current, the power level drained from the cell and whether the discharge is constant or pulsed.

2.1 Notations and Definitions

A *cell* is characterized by three voltage values: (i) the open-circuit voltage (V_{OC}), i.e., the initial value of voltage of the fully charged cell under no-load conditions; (ii) the operating voltage of the cell under load conditions expressed as volt and denoted by V ; (iii) the cut-off voltage at which the cell is considered discharged, denoted by V_{cut} (namely 80% of the V_{OC}). Two parameters are used to represent the cell capacity: the *theoretical* and the *nominal* capacity. The former is based on the amount of active materials contained in the cell and is expressed in terms of ampere-hours. The latter represents the ampere-hours obtained from a cell when it is discharged at a specific constant current to a specific cut-off voltage.

Finally, to measure the cell discharge performance the following parameters are considered. *Discharge time* (t_d) expressed as seconds elapsed until a fully charged cell reaches the V_{cut} voltage and has to be replaced or recharged. *C rate*, i.e., the discharge current equal in ampere to the nominal ampere-hour capacity of the cell; it can be also reported as

current density (ampere per cm^2). Multiple or fractions of the C rate can be used to indicate higher or lower currents. *Specific power (energy)* is the power (energy) expressed as watt (watt-hour) per kilogram delivered by a fully charged cell at a specified current of discharge.

To clarify the above definitions, Fig. 2 from [6] shows the constant current discharge behavior of a lithium-ion cell with $V_{OC}=3$ V and $V_{cut}=1.0$ V.¹ The three curves in the plot correspond to different values of the discharge current.

2.2 Capacity as a Function of the Discharge Current and Power

The electrical current obtained from a cell results from electrochemical reactions occurring at the electrode-electrolyte interface [13, 17, 5]. At zero current, the concentration of the active species in this area of the cell is uniform and equal to its average value; at current greater than zero, the active species are consumed at the electrode-electrolyte interface by electrochemical reactions, and replaced by new active materials that move from the electrolyte solution to the electrode through *diffusion*. However, as the intensity of the current is increased, polarization effects take place, i.e., deviation from the average concentration at the electrode-electrolyte interface become more significant. As a consequence, the state of charge of the electrode as well as the cell voltage decrease. Above a threshold value, called the *limiting* current, the diffusion phenomenon is unable to compensate for the depletion of active materials and, very quickly the concentration of active materials drops to zero at the cathode. At this point, the cell voltage drops below the cut-off value, and, even if the theoretical capacity of the cell has not been exhausted (since active species inside the cell are not exhausted), the cell is considered discharged.

Therefore, a high specific energy (viz. several hundred Wh/kg), can be obtained only if a low specific power (less than 200 W/kg) is drawn. For example, in lead acid batteries with nominal capacity equal to 5 Ah, the delivered capacity increases by 50% if a $C/20$ rate (equal to 250 mA) of constant discharge is used instead of $C = 5A$. Likewise, for lithium-ion batteries the delivered capacity increases by 60% if the constant discharge rate is reduced from 1 A to 125 mA [13]. However, notice that even if a favorable rate of discharge is used, typically the capacity delivered by a battery under constant discharge is only 10-30% of the theoretical value. The discharge time, and the specific energy of a cell under constant discharge can be derived as functions of the drained

¹Permission to reproduce Figure from [6] has not been obtained at this time.

Cell type	K	h
lead acid	73	1.37
sintered Ni-Cd	23.4	1.06
Ni-Fe alkaline	105	1.02

Table 1: Values of the constants K and h characterizing the behavior of some commercial secondary cells.

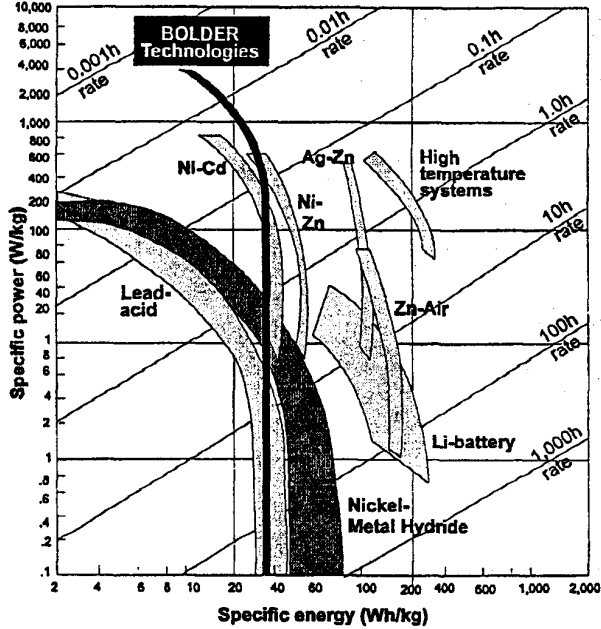


Figure 3: Ragone plots for various battery chemistries.

current by using Peukert's formula [13],

$$t_l = KI^{-h} \quad (1)$$

where K , and h are constants depending on the cell design and chemical structure. In Tab. 1 values of K and h , valid over a large range of discharge currents, are reported for some commercial rechargeable batteries [19]. From (1) and considering a constant voltage, V_a , equal to the average value of the cell voltage during the discharge, the specific energy results that

$$E = V_a \cdot I \cdot t_l = V_a \cdot KI^{1-h} \quad (2)$$

Eqs. (1) and (2) show the non-linear behavior of batteries: increasing I by a factor α , the cell discharge time and the specific energy result reduced by a factor equal to α^h and α^{h-1} , respectively. In Fig. 3, a log-log plot of the specific power versus the specific energy, known as Ragone plot, is shown for different commercial rechargeable batteries.² The left leaning curves show the inverse relationship between specific energy and specific power.

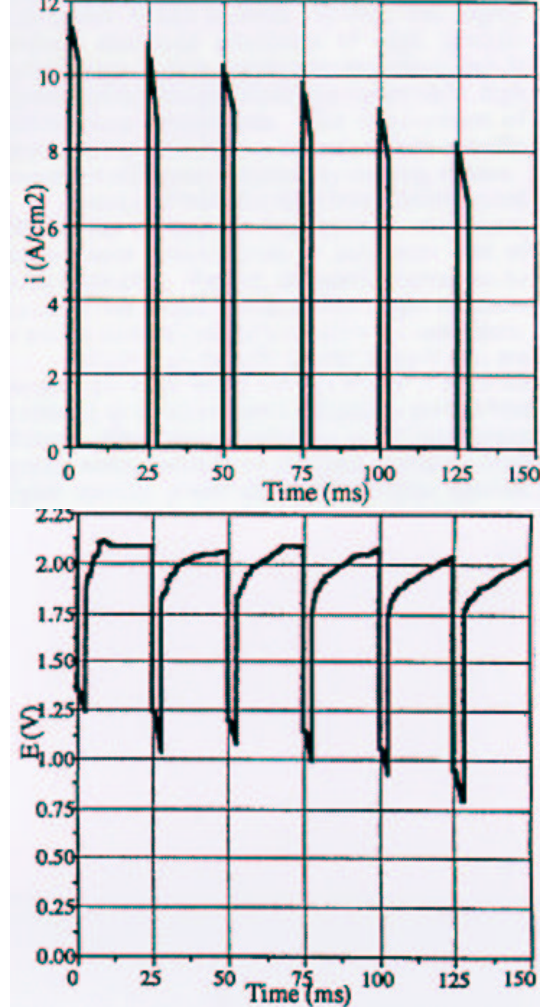


Figure 4: Performance of a bipolar lead-acid cell subjected to six current impulses. Pulse length=3 ms, rest period=22 ms.

2.3 Effect of Pulsed Discharge

Some of the limitations presented by the constant current discharge process can be overcome when pulsed current discharge is used. If after draining an impulse of current the cell is allowed to relax long enough, then the concentrations gradient decreases and a charge recovery takes place at the electrode. As already mentioned, this effect is due to the diffusion process that compensates for the depletion of the active materials allowing the cell to achieve again a value of voltage equal to V_{OC} . Moreover, since polarization phenomena are more pronounced at heavier loads, the recovery effect is more significant as the current drained from the cell increases [13, 5].

These benefits still hold in the case of a discharge process characterized by impulses superimposed on a *background* current [10, 12]. Such discharge patterns are likely in communication devices where the baseband and RF parts need a constant background supply, but load changes occur when-

²Permission to reproduce Figure from [16] has not been obtained at this time.

ever the system passes from the idle to the active state or the radio transceiver switches from receive to transmit mode. Several results are present in the literature [13, 8, 11, 10] illustrating the advantages that result from a pulsed current discharge. In [8], a lithium-ion cell with an initial specific power equal to 600 W/kg, experienced a constant discharge to 80% depth of discharge, then a power impulse 30 s long was drawn off the cell. The drained specific peak power significantly grew as the rest period duration after the constant discharge increased: from 320 W/kg for no rest period, a value of 490 W/kg was obtained for a rest period 20 min. long. A Sony phone cell with nominal capacity equal to 1 Ah was subjected to a discharge at 1.9 A for 16 min., and it was observed that after a rest period 20 min. long the cell voltage was again very close to the initial value. We point out that the discharge time in these experiments are much longer than the typical timing used in radio communications systems; however, these results clearly prove that the delivered specific energy can be increased by using a pulsed discharge instead of a constant discharge.

Referring to experiments that involve more suitable values of discharge time, in [11] a bipolar lead-acid cell was subjected to six current impulses each of them lasting 3 ms and followed by a rest period 22 ms long. Fig. 4 shows the results of this experiment.³ The drained current was initially equal to 12 A/cm² and dropped to 7 A/cm² at the end of the sixth impulse. During the first 4 rest periods, the cell was able to totally recover the initial value of voltage, and it was observed that, since the total consumed active material was less than the 50%, a minor decrease of performance would have occurred during the last two impulses if a longer rest period had been allowed. This result suggests that in order to increase the specific energy obtained from the cell, the recovery period should be increased as the discharge depth becomes greater.

Referring to the TMF technology [17, 16], an experiment was done in which a cell was discharged at 6 V, both at a constant current equal to 100 A and at 100 A current impulses lasting 1 s and followed by a rest period 1 s long. The delivered capacity from the former discharge mode was 0.44 Ah, from the latter 0.5 Ah, i.e., the gain obtained using a pulsed discharge with respect to a constant current discharge at comparable current levels was about 13.6%. However, even under a pulsed discharge the delivered capacity was only 41.7% of the theoretical cell capacity. Perhaps even higher gains can be expected from the pulsed discharge of the cell if a longer rest period is considered.

In batteries characterized by a relatively low conductivity, e.g., lithium-polymer cells [2, 9], pulsed discharge can increase the delivered specific power. Lithium-polymer cells have lightweight and flat formats and fit well in extra-thin cellular phones, but ion diffusion through the conducting polymers is slow and this limits the rate at which current can be withdrawn from a cell. However, in [4] a lithium-polymer cell was discharged at up to 50 mA/cm², about fourteen times the typical constant discharge rate, using pulses of 10 ms duration followed by a 50 ms rest period.

2.4 Passivation Effects

Another effect, called passivation, has to be taken into account in the cell behavior under both constant and pulsed

current discharge. Indeed, the cell discharge time may be limited not only by the diffusion process, but also by the precipitation of crystals, produced by the discharge electrochemical reactions on the electrode. This passivation effect is faster for high current densities. For extremely high values of current, a rapid decrease of the cell voltage occurs due to the passivation effect.

In [10], lead-acid cells were studied under a pulsed discharge of 2 ms and with current density starting from 15 A/cm². It was shown that during the first 100 μ s, the concentration gradients of the active species are the major cause of the decrease of the drained current density, whereas after 100-200 μ s passivation phenomena begin, determining a sharp drop of the current density after 200 μ s. However, for these cells typical values of the limiting current density are tens of mA/cm². Such a low passivation time constant was observed by applying a current about three orders of magnitude greater than the limiting current; whereas, typically passivation time constants are much greater than 200 μ s.

2.5 Summary of Battery Behavior

Summarizing, the advantage of pulsed current discharge is twofold:

- i) For a fixed power level, the delivered specific energy is greater if a pulsed discharge is used. With pulsed discharge, the active materials at the electrode-electrolyte interface are partially recovered depending on the drained power and on how long the idle periods are. Ideally, the cell would be exhausted only when all the active materials in the cell have been exploited.
- ii) By using a pulsed discharge, a higher specific power can be drained from the cell for a constant delivered specific energy. In fact, by properly choosing the impulse and the idle time duration, impulses of amplitude equal to several times the limiting current value can be obtained.

3 Performance of Cells under Pulsed Discharge

In this section, we analyze the stochastic evolution of a cell from the fully charged to the completely discharged state. Discharges occur at stochastic instants determined by a Bernoulli process and recovery occurs whenever there is no discharge. In order to estimate the improvements from a pulsed current discharge relative to a constant current discharge, the average number of packets transmitted in both the operational conditions are computed and compared.

To carry out our analysis, the following assumptions are made:

- i) A single cell of the battery system is considered; however, the results can be easily extended to the case of several cells connected in series or in parallel;
- ii) The time constant of the passivation phenomenon is assumed to be greater than the discharge time necessary to drain the theoretical capacity of the cell, and therefore passivation effects are neglected;
- iii) A discrete time system with time unit equal to one frame duration is considered;

³Permission to reproduce Figure from [11] has not been obtained at this time.

Supplies required			
Baseband/Digital	3.3 V	200 mA	
RF	3-5 V	100 mA	
Power Amplifier	3-6V	1.2-1.5 A ⁴	
System	Duty cycle	Frame	Slot
GSM	1:8	4.6 ms	577 μ s
PACS	1:8	2.5 ms	313 μ s
DECT	1:24	10 ms	41.7 μ s

Table 2: Power consumption and time frame characterizing radio systems currently used; the duty cycle value represents the ratio of the slot to the frame duration.

- iv) For the sake of simplicity the background current (see Sect. 2.3) is neglected; only the amount of capacity necessary to transmit a packet is considered and defined as a *charge unit*;
- v) Each fully charged cell has a theoretical capacity equal to T , and a nominal capacity equal to N *charge units* when it is discharged at a constant current. Both N and T vary for different kinds of cell; moreover, N also depends on the discharge rate.

Two different pulsed discharge modes are considered:

- *Binary pulsed discharge*: in each time frame the system transmits a packet if there is any, otherwise it recovers one charge unit. In case of transmission, the supply required by the power amplifier is obtained by draining current during the entire duration of the time frame.
- *Generalized pulsed discharge*: in each time frame the system may transmit one or more packets, or recover charge. The impulse amplitude is equal to the current required by the power amplifier times the number of transmitted packets, while the impulse duration is equal to a fraction of the time frame (slot). The remaining time of the frame duration permits the recovery of one charge unit.

In both the pulsed discharge modes the recovery process ends once the theoretical capacity is exhausted. Typical values of the frame duration and the required current in modern radio systems are reported in Tab. 2 [14]; the value of the charge unit can be easily computed. In GSM systems one charge unit results equal $1.2A \cdot 577\mu s = 0.192 A\mu s$. Experiments executed on lead-acid and lithium-ion batteries considering similar values of duty cycle and frame duration can be found in the literature [11, 10, 17].

3.1 Binary Pulsed Discharge

The cell behavior is modeled as a transient process that starts from the state of full charge ($V = V_{OC}$), denoted by N , and terminates when the state 0 (corresponding to a complete discharge of the cell) is reached, or the theoretical capacity is exhausted. Fig. 5 shows a graphical representation of the process, where a *dummy* state, N_s , was added to represent the start of discharge. The packet arrival process is assumed to be Bernoulli with probability $a_1 = q$ that one packet arrives in a time frame. Thus, in each time frame a

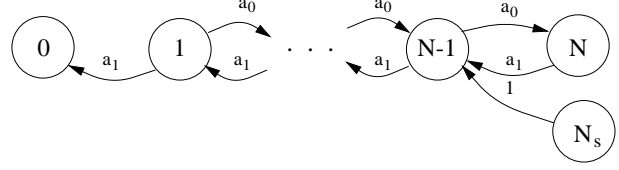


Figure 5: Binary Markov chain representing the cell behavior.

packet transmission occurs with probability a_1 , while a recovery takes place with probability $a_0 = (1 - q)$. Notice that while 0 is a trapping state, N may be reached more than once due to the recovery process; however, the charge state of the cell can never exceed N .

Let us denote by $m_{z,0}(n)$ the number of packet transmissions made when the process starts from state z ($0 < z < N$) and reaches the final state 0 in n steps. Then, for a given T and $z = N - 1$, the number of transmitted packets is equal to $(1 + m_{N-1,0}(n)) \leq T$ if the cell process reaches state 0 at the time instant n before the theoretical capacity is completely consumed, and equal to T , otherwise.

We define $u_{z,0}(n)$ as the probability to reach state 0 in n steps starting from state z ($0 < z < N$) and we derive $u_{z,0}(n)$ for $n \geq 1$, considering that the following boundary conditions hold

$$\begin{aligned} u_{z,0}(n) &= 0 & n &\geq 1 \\ u_{z,0}(0) &= 1, \quad u_{z,0}(0) = 0 & 0 < z \leq N. \end{aligned}$$

Referring to Fig. 5, we can write

$$u_{z,0}(n) = a_0 u_{z+1,0}(n-1) + a_1 u_{z-1,0}(n-1) \quad 0 < z < N \text{ and } n \geq 1. \quad (3)$$

Moreover,

$$\sum_{n=0}^{\infty} u_{z,0}(n) = 1. \quad (4)$$

Using the method of generating functions, then solving the system of linear equations and anti-transforming [7], we obtain for $z = N - 1$

$$\begin{aligned} u_{N-1,0}(n) &= \frac{2^n}{A_n(N+1)} a_0^{\frac{n-N+1}{2}} a_1^{\frac{n+N-1}{2}} \sum_{i=1}^N \cos^{n-1} \frac{\pi i}{N+1} \\ &\quad \sin \frac{\pi i}{N+1} \sin \frac{\pi i(N-1)}{N+1} \end{aligned} \quad (5)$$

with A_n being the following normalization constant

$$A_n = \begin{cases} 1 - \frac{1 - \left(\frac{a_1}{a_0}\right)^N}{1 - \left(\frac{a_1}{a_0}\right)^{N+1}} & \text{if } a_0 \neq \frac{1}{2} \\ \frac{2}{N+1} & \text{if } a_0 = \frac{1}{2} \end{cases} \quad (6)$$

$$(7)$$

By substituting the expression (5) in (3), equation (3) is satisfied. Also, as expected, $u_{N-1,0}(n) = 0$ when $n - N + 1$ is odd and for $n < N - 1$.

⁴Peak value requested during a packet transmission.

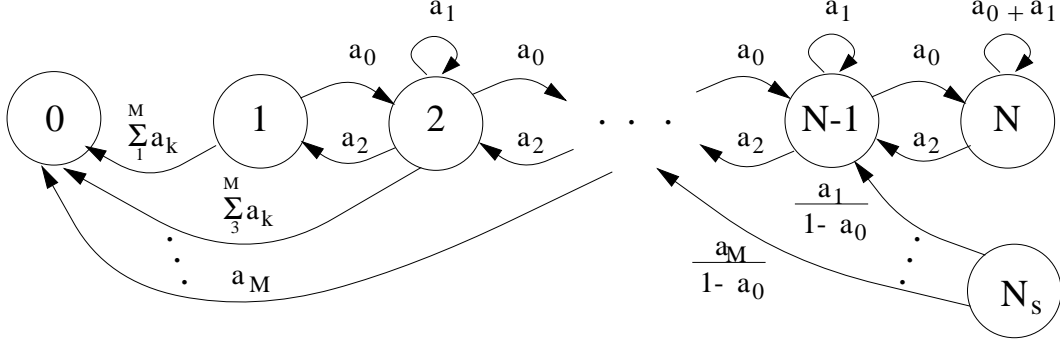


Figure 6: Markov chain representing the cell behavior in case of generalized pulsed discharge.

Since each backward step in the Markov chain shown in Fig. 5 corresponds to a packet transmission, by examining the exponent of a_1 in (5), we derive

$$m_{N-1,0}(n) = \frac{n + N - 1}{2} \quad n \geq N - 1. \quad (8)$$

Thus the probability to reach 0 before the capacity T is exhausted, is

$$f_{N-1,0}(T) = \sum_{n=1}^{2T-N-1} u_{N-1,0}(n) \quad (10)$$

where $(2T - N - 1)$ is the maximum number of steps that allow to reach 0 before the theoretical capacity ends. By writing

$$m_{N-1,0}^* = \sum_{n=1}^{2T-N-1} \frac{n + N - 1}{2} u_{N-1,0}(n) \quad (11)$$

the total expected number of transmitted packets is derived as

$$\bar{m}_p = 1 + m_{N-1,0}^* + [1 - f_{N-1,0}(T)](T - 1) \quad (12)$$

where, the unitary value takes into account the packet transmitted upon the process starts. Finally, we assume that the charge units drained from a cell under a constant discharge can be fully utilized by accumulating charge in a capacitor whenever it needs. Thus, by defining the gain G obtained from a pulsed discharge relative to a constant discharge as the ratio of the mean number of transmitted packets under the two discharge methods, we have

$$G = \frac{\bar{m}_p}{N}. \quad (13)$$

G can be at most equal to T/N . Pulsed discharge outperforms the constant current discharge to the extent that G exceeds 1 and approaches T/N .

3.2 Generalized Pulsed Discharge

In this case, arrivals of bursts of packets are considered. We define a_k as the probability that a burst arrival contains

k packets, and M as the maximum number of packets per burst, that for the sake of simplicity, is assumed less than or equal to N . Thus, the average number of packets that arrive in a time frame is given by

$$q = \sum_{k=1}^M k a_k \quad (14)$$

while the probability to recover is equal to $a_0 = 1 - \sum_{k=1}^M a_k$. Now, in each time frame the cell has probability a_k to move from state z to $z - k + 1$, with $0 < z < N$, where the positions corresponding to $z - k + 1 < 0$ add to the probability to move to 0. The Markov chain associated with the cell behavior is presented in Fig. 6.

The probability to reach 0 in n steps starting from state z can be derived following the same procedure used in the analysis of the binary pulsed discharge (see Sect. 3.1). Now, the linear system to be solved is

$$u_{1,0}(n) = a_0 u_{2,0}(n-1) + \sum_{k=1}^M a_k \delta(n-1) \quad n \geq 1 \quad (15)$$

$$u_{z,0}(n) = \sum_{k=0}^M a_k u_{z-k+1,0}(n-1) \quad 1 < z < N - 1, n \geq 1 \quad (16)$$

$$u_{N,0}(n) = (a_0 + a_1) u_{N,0}(n-1) + \sum_{k=2}^M a_k u_{z-k+1,0}(n-1) \quad n \geq 1 \quad (17)$$

with the following boundary conditions

$$\begin{aligned} u_{x,0}(0) &= 1, & u_{x,0}(n) &= 0 & n &\geq 1 \text{ and } x \leq 0 \\ u_{x,z}(n) &= 0 & n &\geq 0, x \leq 0, \text{ and } 1 \leq z \leq N. \end{aligned}$$

In addition, the normalization equation (4) must still hold. Since in this case it is cumbersome to anti-transform the generating functions, an approximation is adopted to numerically compute $u_{z,0}(n)$. Relative to the Markov chain shown in Fig. 6, a chain slightly different at the border states 0 and N is considered. For $N=3$ the approximated values are quite close to the exact results, and the approximation becomes more satisfactory as N increases.

In deriving the number of packets transmitted in n steps, we must take into account that each backwards k -step jump corresponds to $k + 1$ transmitted packets. Moreover, from state N_s , M possible states may be reached at the start time instant. Then, using (10) and (11) conditioned this time on all the possible initial states ($N - M < z < N - 1$), we can compute $f_{N-k,0}(T)$ and $m_{N-k,0}^*$ ($k=1, \dots, M$), respectively. Based on this approach the following is derived

$$G = \frac{1}{N} \cdot \sum_{k=1}^M \frac{a_k}{1 - a_0} \{k + m_{N-k,0}^* + [1 - f_{N-k,0}(T)](T - k)\}. \quad (18)$$

4 Results

By using the analytical expressions derived in Sect. 3, the gain G is computed as a function of q , i.e., the average number of packets that arrive in one time frame. Assuming the same frame duration for all the considered cases, the binary and the generalized pulsed discharge performance is presented. From Fig. 7, it can be seen that performance

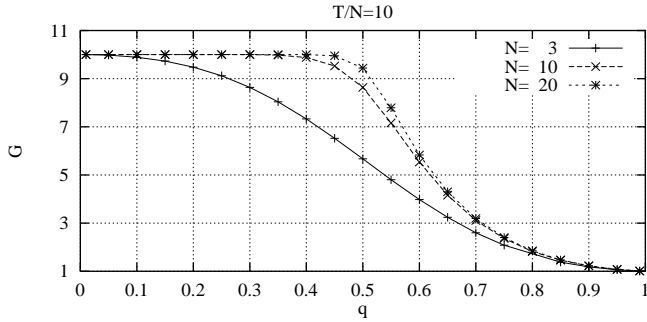


Figure 7: G vs. q for binary pulsed discharge as N varies, and $T/N = 10$.

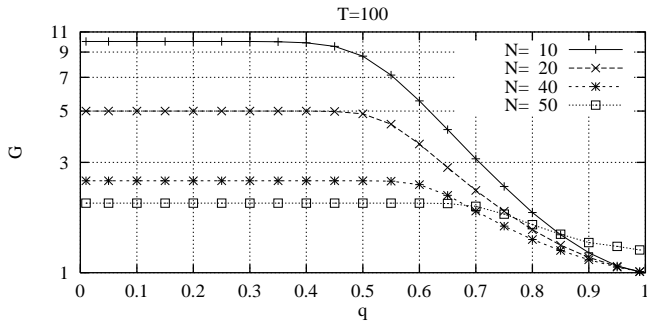


Figure 8: Gain obtained in the case of binary pulsed discharge with $T=100$, and N varying. G is represented in logarithmic scale.

gains are most significant for low values of q , i.e., when the cell has more chance to recover. On the other hand, even for high values of N , when q becomes greater than 0.5, the gain obtained using the binary pulsed discharge decreases until it reaches the lower bound value equal to 1. In this

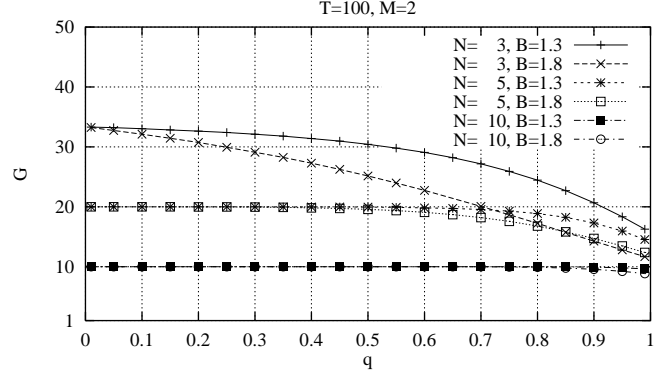


Figure 9: Gain obtained in the case of generalized pulsed discharge with $T=100$, $M=2$, and B and N varying.

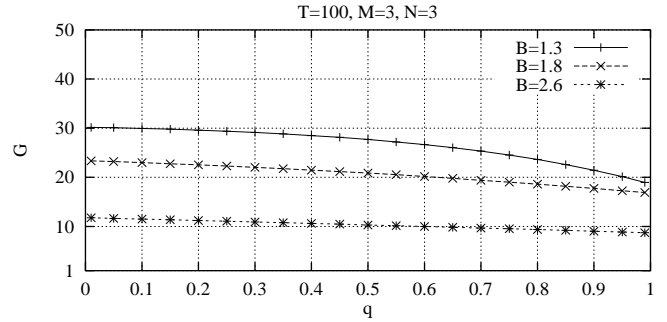


Figure 10: Gain obtained in the case of generalized pulsed discharge with $T=100$, $M=3$, $N=3$, and B varying.

case, pulsed and constant current discharge give the same performances. As shown in Fig. 8 holding T constant and varying N , we notice that the theoretical capacity cannot be completely exploited at high values of q ; however, for N approaching 50% of T , the gain is always greater than 1. A significant improvement is achieved in the generalized pulsed discharge mode, i.e., by letting the battery recover more often. In this case, it is useful to define B as the average burstiness of the packet arrival process:

$$B = \sum_{k=1}^M k \frac{a_k}{1 - a_0}. \quad (19)$$

Given B and q , and using (14) and (19), the values a_k ($k=0,1,\dots,M$) are derived accordingly. Fig. 9 shows that for N equal to the 10% of T , larger values of G are obtained by using the generalized pulsed discharge even at high packet arrival rates. However, it is interesting to notice that for $M = 2$ and small values of N , G sensibly decreases when the value of B changes from 1.3 to 1.8.

This effect is confirmed by the plot in Fig. 10, where the G behavior versus q is presented for $T=100$, $M=N=3$, and different values of B . It can be seen that as B increases, performances become worse even for small values of q . This suggests that in order to efficiently deliver bursts of power, the initial state of charge of the cell must be sufficiently greater than the maximum burst size, or a traffic control policy has to be adopted to let the battery properly recover.

5 Conclusions and Future Work

The paper presented the most interesting aspects of the battery behavior that can be exploited to improve battery lifetimes. An analysis of the single cell performance was carried out and results proving the actual benefits of the pulsed discharge were shown. The major lesson learned from this study is: *i*) Battery performances greatly improve as the probability to recover increases; *ii*) in order to efficiently deliver bursts of power, the initial state of charge of the cell must be sufficiently greater than the maximum burst size; *iii*) traffic control techniques should be investigated and proper schemes implemented for more efficient battery management.

Further work should be done to get a better understanding of the recovery phenomenon, so that for every value of discharge current and battery type the required relaxation time period is estimated. The challenge will be to find ways to shape the actual discharge demand process to better conform to the optimal discharge profile. It is our belief that the discharge shaping will be performed primarily by delaying some power consuming activity such as transmission of a packet. Intuitively, it seems clear that the fundamental tradeoff here is between delay and energy efficiency.

References

- [1] N. Bambos, J.M. Rulnick, "Mobile Power Management for Maximum Battery Life in Wireless Communication Networks," *Proc. IEEE Infocom'96*, Mar. 1996, pp. 443-450.
- [2] P. Calvert, *et al.*, "Pyrrole Copolymers with Enhanced Ion Diffusion Rates for Lithium Batteries," *MRS Symposium Proceedings*, vol. 496, Dec. 1997, Boston, pp. 485-491.
- [3] J.C. Chen, *et al.*, "On Scheduling of Multimedia Services in a Low-Power MAC for Wireless ATM Networks," *PIRMC'98*, Sept. 1998.
- [4] H.S. Choe, K.M. Abraham, "Synthesis and Characterization of LiNiO_2 as a Cathode Material for Pulse Power Batteries," *MRS Symposium Proceedings*, vol. 496, Dec. 1997, Boston, pp. 303-308.
- [5] M. Doyle, J. Newman, "Analysis of capacity-rate data for lithium batteries using simplified models of the discharge process," *Jo. Applied Electrochem.*, vol. 27, no. 7, July 1997, pp. 846-856.
- [6] Duracell OEM, "Lithium Manganese Dioxide. Performance Characteristics," <http://www.duracell.com/OEM/index.html>.
- [7] W. Feller, *An Introduction to Probability Theory and Its Applications*, 3rd Ed., John Wiley & Sons, New York, 1968.
- [8] T.F. Fuller, M. Doyle, J. Newman, "Relaxation phenomena in lithium-ion-insertion cells," *Jo. Electrochem. Soc.*, vol. 141, no. 4, Apr. 1994, pp. 982-990.
- [9] J.W. Halley, B. Nielsen, "Simulation Studies of Polymer Electrolytes for Battery Applications," *MRS Symposium Proceedings*, vol. 496, Dec. 1997, Boston, pp. 101-107.
- [10] R.M. LaFollette, D. Bennion, "Design Fundamentals of High Power Density, Pulsed Discharge, Lead-Acid Batteries. II Modeling," *Jo. Electrochem. Soc.*, vol. 137, no. 12, Dec. 1990, pp. 3701-3707.
- [11] R.M. LaFollette, "Design and Performance of High Specific Power, Pulsed Discharge, Bipolar Lead Acid Batteries," *10th Annual Battery Conference on Applications and Advances*, Long Beach, Jan. 1995, pp. 43-47.
- [12] B. Le Pioufle, J.F. Fauvarque, P. Delalande, "Comportement non linéaire des générateurs électrochimiques associés aux convertisseurs statiques. Détection de l'état de charge," *The European Physical Journal. Applied Physics*, vol. 2, no. 3, June 1998, pp. 257-265.
- [13] H.D. Linden, *Handbook of Batteries*, 2nd ed., McGraw-Hill, New York 1995.
- [14] T. Millward, "Power Supply Design. A Brief Tutorial," IEE Publisher, London 1998.
- [15] B. Narendran, *et al.*, "Evaluation of an Adaptive Power and Error Control Algorithm for Wireless Systems," *IEEE Int. Conf. on Comm.*, 1997, pp. 349-355.
- [16] B. Nelson, "TMF ultra-high rate discharge performance," *12th Annual Battery Conference on Applications and Advances*, Long Beach, Jan. 1997, pp. 139-143.
- [17] B. Nelson, R. Rinehart, S. Varley, "Ultrafast pulse discharge and recharge capabilities of thin-metal film battery technology," *11th IEEE International Pulsed Power Conference*, Baltimore, June 1997, pp. 636-641.
- [18] E.J. Podhala, H.Y. Cheh, "Modeling of Cylindrical Alkaline Cells. VI: Variable Discharge Conditions," *J. Electrochem. Soc.*, vol. 141, no. 1, Jan. 1994, pp. 28-35.
- [19] S.M. Selis, C.R. Russell, "An Analytic Representation of Discharge Characteristics of Commercial Secondary Batteries," *Jo. of Electrochem. Soc.*, vol. 1, no. 3-4, Mar.-Apr. 1963, pp. 77-81.
- [20] J.S. Shauh, R.R. Rao, "A Power Efficient Zone Based Resource Assignment (ZBRA) Scheme for Wireless Communications," *ICUPC'98*, Florence, Italy, June 1998.
- [21] M. Zorzi, R.R. Rao, "Error Control and Energy Consumption in Communications for Nomadic Computing," *IEEE Trans. on Comp.*, vol. 46, no. 3, Mar. 1997, pp. 279-289.